Available online at www.sciencedirect.com
ScienceDirect
International Journal of Heat and Fluid Flow 29 (2008) 1197–1202
International Journal of HEAT AND FLUID FLOW
www.elsevier.com/locate/ijhff

Simulation of heat transfer in a ferrofluid using computational fluid dynamics technique

A. Jafari [a,*], T. Tynjälä [a], S.M. Mousavi [b,c], P. Sarkomaa [a]

[a] Laboratory of Engineering Thermodynamics, Lappeenranta University of Technology, Lappeenranta, Finland
[b] Biotechnology Group, Chemical Engineering Department, Tarbiat Modares University, P.O. Box 14115-143,Tehran, Iran
[c] Department of Chemical Engineering, Lappeenranta University of Technology, Lappeenranta, Finland

Received 10 September 2007; received in revised form 22 November 2007; accepted 7 January 2008
Available online 3 April 2008

Abstract

In the present work computational fluid dynamics (CFD) was used to study heat transfer phenomena in a kerosene based ferrofluid. The flow behaviour was investigated in two cylinders with different dimensions, and the ferrofluid was treated as a two phase mixture of magnetic particles in the carrier phase. Different temperature gradients and uniform magnetic fields were applied over the geometries. Numerical results illustrate that the transport processes in the presence of magnetic field will enhance in comparison with the field free case. In addition obtained results show that in the presence of aggregation of magnetic particles heat transfer will decrease, and Rayleigh rolls will not be observed. It was also shown that when magnetic field is perpendicular to the temperature gradient, the heat transfer will increase more compare to the case with magnetic field parallel to temperature gradient.

Keywords: CFD simulation; Heat transfer; Ferrofluid

1. Introduction

Ferrofluids are composed of magnetic nanoparticles and carrier fluid (Xuan et al., 2005). Such fine particles may be coated by a suitable surfactant to keep a stable suspension state and they can be treated as particles of single magnetic domain. But some particles may combine to each other because of dipole-dipole interactions, and aggregations will produce (Tynjälä et al., 2006).

Ferrofluids are a type of functional fluids whose flow and energy transport processes can be controlled by adjusting an external magnetic field, which makes it find a variety of applications in various fields. For example using ferrofluids in miniaturized devices and external magnetic field enhance convection in these devices (Strek and Jopek, 2007).

Study of transport phenomena in ferrofluids involves use of computational fluid dynamics (CFD). Several recent publications have established the potential of CFD for describing the ferrofluids behaviour like fluid motion and heat transfer (Tynjälä and Ritvanen, 2004; Snyder et al., 2003; Tynjälä et al., 2002; Tangthieng et al., 1999). The relationship between an imposed magnetic field, the resulting ferrofluid flow and the temperature distribution is not understood well enough, and the references regarding heat transfer with magnetic fluids is relatively sparse (Strek and Jopek, 2007). In this work heat transfer of a kerosene based ferrofluid in cylindrical geometries under influence of magnetic field strength was simulated. In addition the influence of magnetic particle's diameter on heat transfer was studied.

2. Governing equations

2.1. Mixture model

Since mixture model can predict the behaviour of ferrofluids (Tynjälä, 2005; Jafari et al., 2007), this method was used to study in this work. The continuity, momentum,

* Corresponding author.
E-mail address: ajafari@lut.fi (A. Jafari).

0142-727X/$ - see front matter © 2008 Elsevier Inc. All rights reserved.
doi:10.1016/j.ijheatfluidflow.2008.01.007

and energy equations for the mixture and the volume fraction equation for the secondary phase, as well as algebraic expressions for the relative velocities are as follow:

$$\frac{\partial}{\partial t}(\rho_m) + \nabla \cdot (\rho_m v_m) = 0 \tag{1}$$

$$\frac{\partial}{\partial t}(\rho_m v_m) + \nabla \cdot (\rho_m v_m v_m) = -\nabla P_m + \mu_m \nabla^2 v_m - \nabla \cdot (\alpha_p \rho_p v_{Mp} v_{Mp} + \alpha_c \rho_c v_{Mc} v_{Mc}) + \rho_m g + \alpha_p \frac{m_p}{V_p} L(\xi) \nabla H \tag{2}$$

$$\frac{\partial}{\partial t}(\rho_m c_{v,m} T) + \nabla \cdot [(\alpha_p \rho_p v_p c_{p,p} + \alpha_c \rho_c v_c c_{p,c}) T] = \nabla \cdot (k_m \nabla T) \tag{3}$$

where ρ, v, P, μ, ξ and k are density, velocity, pressure, dynamic viscosity, Langevin parameter and conductivity, respectively. The subscripts m, p and c refer to the mixture, magnetic particles and carrier fluid, respectively and $v_{Mi} = v_i - v_m$ is diffusion velocity. Using the continuity equation, the volume fraction equation for magnetic phase can be obtained:

$$\frac{\partial}{\partial t}(\alpha_p \rho_p) + \nabla \cdot (\alpha_p \rho_p (v_m - v_{dr,p})) = 0 \tag{4}$$

where $v_{dr,p}$ is drift velocity. With considering to forces act on a single magnetic particle, the slip velocity is defined similar to Jafari et al. (2008):

$$v_s = v_p - v_c = \frac{m_p L(\xi)}{3\pi\mu_c d_p} \nabla H + \frac{d_p^2 (\rho_p - \rho_c)}{18\pi\mu_c} g \tag{5}$$

where d_p is the magnetic particle diameter.

2.2. Magnetic field calculation

The conductivity of ferrofluids is usually very small, so Maxwell's equations are as follow:

$$\nabla \cdot B = 0, \tag{6}$$

$$\nabla \times \mathbf{H} = 0, \tag{7}$$

where $\mathbf{B}$ is the magnetic induction, and $\mathbf{H}$ is the magnetic field vector. Further the magnetic induction, the magnetization vector, $\mathbf{M}$, and the magnetic field vector are related by the constitutive relation:

$$\mathbf{B} = \mu_0(\mathbf{M} + \mathbf{H}), \tag{8}$$

where μ_0 is a magnetic permeability in vacuum. Magnetic scalar potential, ϕ_m, is defined as:

$$\mathbf{H} = -\nabla \phi_m. \tag{9}$$

Using Maxwell's equations, the flux function for magnetic scalar potential, ϕ_m may be written as:

$$\nabla \cdot \left[\left(1 + \frac{\partial \mathbf{M}}{\partial \mathbf{H}} \nabla \phi_m \right) \right] = \nabla \cdot \left[\left(\frac{\partial \mathbf{M}}{\partial T}(T - T_0) + \frac{\partial \mathbf{M}}{\partial \alpha_p}(\alpha_p - \alpha_{p_0}) \right) \right] \tag{10}$$

where α_p, T and subscript 0 represent the volume fraction of magnetic particles, temperature and initial conditions, respectively. Within the simulations $\frac{\partial \mathbf{M}}{\partial \mathbf{H}} = \chi$, $\frac{\partial \mathbf{M}}{\partial T} = -\beta_m \mathbf{M}_0$ and $\frac{\partial \mathbf{M}}{\partial \alpha_p}$ are assumed to be constant and using Langevin equation they can be defined (Jafari et al., 2008).

3. Numerical methods

Commercial software, Gambit, was used to create the geometries (cylinder 1 with both height and diameter of 10 mm and cylinder 2 with height and diameter of 3.5 mm and 75 mm, respectively) and generate the grids. Fig. 1a depicts a schematic of cylinder 1 used in the simulations and the related grid is illustrated in Fig. 1b. Fig. 2 shows the grid for cylinder 2. To divide the geometries into discrete control volumes, about 5.9×10^5 and 10^5 tetrahedral computational cells, 1.2×10^6 and 2×10^5 triangular elements, and more than 10^5 and 2.4×10^4 nodes were used for cylinder 1 and 2, respectively.

A grid independency check has been performed for both cylinders. Temperature difference 100 K and magnetic field strength 160 kA/m parallel to the temperature gradient were applied over cylinder 1. Concentration difference of dispersed phase or separation after 100 s was considered to compare grids, and results have been shown in Table 1.

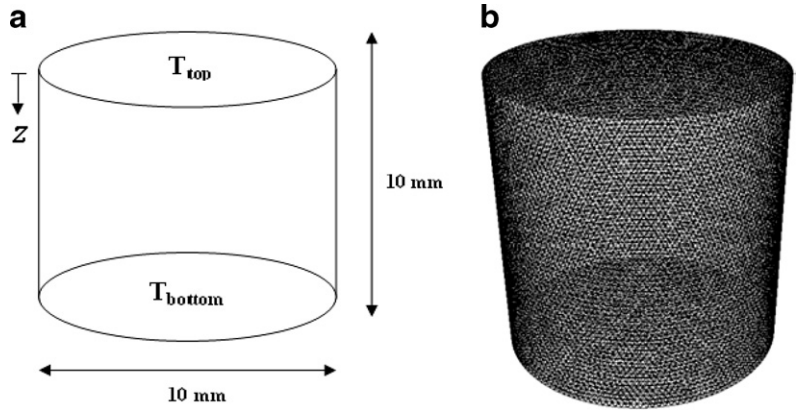

Fig. 1. (a) Schematic of cylinder 1, (b) the grid related to the geometry with aspect ratio 1.

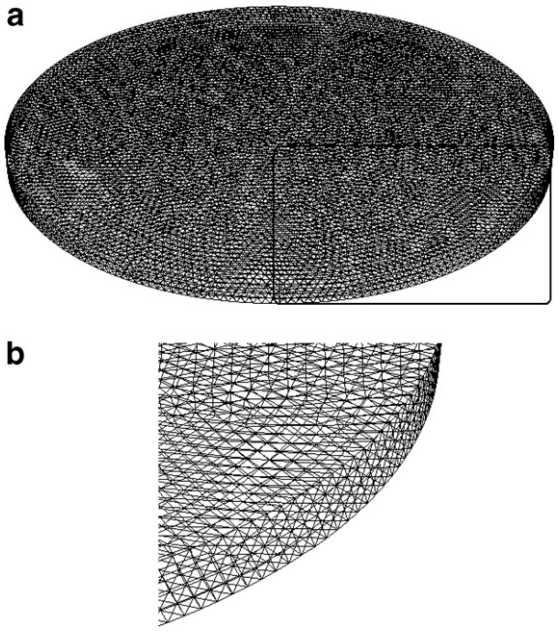

Fig. 2. (a) The grid used for the cylinder with diameter and length of 75 mm and 3.5 mm, respectively. (b) To obtain better visualization the highlighted part in Fig. 2a is magnified.

Table 1
Percentage of phase separation at different grids in cylinder 1

Grid	1	2	3
Numerical results (percent of concentration difference of dispersed phase)	6.5	9.5	9
Number of tetrahedral elements	10^5	5.9×10^5	1.3×10^6
Number of nodes	1.9×10^4	10^5	2.3×10^5

As the difference between numerical results in grids 2 and 3 is less than 6%, so to save cost and time grid 2 was chosen for all of tests.

For the second cylinder also three different grids have been chosen. Their details and obtained numerical results at $M_s = 48$ kA/m, $d = 5.5$ nm, $\Delta T_{critical} = 25$ K and $\Delta T_{critical} = 25$ K are shown in Table 2. The results appear to be grid independent. There was no significant variation in the Nusselt number resulted by the grid with 2.1×10^5 mesh volume and those obtained from the fine grid, so the second grid was selected for all calculations.

The commercial code for computational fluid dynamics, Fluent, has been used for the simulations, and a user defined function (UDF) was performed to obtain a uniform external magnetic field parallel to the temperature gradient. The finite volume method was adopted to solve three dimensional governing equations. The solver specifications for the discretization of the domain involve the presto, second-order upwind and first-order upwind for pressure, momentum and volume fraction, respectively. In addition second-order upwind was used for energy. Constant temperature boundary conditions were applied for both bottom and top of the cylinders. The under-relaxation factors, which are significant parameters affecting the convergence of the numerical scheme, were set to 0.3 for the pressure, 0.7 for the momentum, and 0.2 for the volume fraction. Using mentioned values for the under-relaxation factors a reasonable rate of convergence was achieved.

Table 2
Effect of second cylinder's mesh on Nusselt number after 200 s

Grid	# 1	# 2	# 3
Number of nodes	1.9×10^3	2.4×10^4	5×10^4
Mesh volume	1.2×10^5	2.1×10^5	2.5×10^5
Nusselt number (Nu)	4.1	1.238	1.234

4. Results and discussion

A kerosene-based magnetic fluid with magnetization 48 kA/m was used in this study. For the sake of simplicity, it is assumed that the effect of the magnetization variation due to the local temperature change of the ferrofluid is negligible because our main attention is to develop a numerical algorithm for the energy transport of a ferrofluid. Such assumption will not alter the intrinsic characteristic of the algorithm, but it simplifies the numerical computation. Other properties of the studied fluid are shown in Table 3. It is assumed that the density of carrier liquid, kerosene, changes with average temperature according to the following equation:

$$\rho_c = 1248 - 1.56 \times T. \tag{11}$$

Properties of the mixture except viscosity can be calculated as follow:

$$N_m = \sum_{i=1}^{i=2} \alpha_i N_i \tag{12}$$

Table 3
Properties of the studied ferriofluid. Here c and p illustrate continuous and dispersed phase, respectively

Property	Value	Property	Value
Density (p)	5400 kg/m^3	Heat capacity at constant pressure (c)	2090 J/kgK
Thermal conductivity (c)	0.149 W/mK	Heat capacity at constant pressure (p)	4000 J/kgK
Thermal conductivity (p)	1 W/mK	Particle magnetic moment	2.5×10^{-19} Am^2
Dynamic viscosity (c)	0.0024 kg/ms	Vacuum permeability	$4\pi \times 10^{-7}$ H/m
Dynamic viscosity (c)	0.03 kg/ms	Thermal expansion coefficient	0.008 1/K

where N represents any property, and i refers to both continuous and dispersed phases. Dynamic viscosity of mixture can be shown as (Rosensweig, 1997)

$$\mu_m = \left(1 + \frac{5}{2}\alpha_{p_0}\right)\mu_c. \quad (13)$$

The temperature difference 10 K was applied to the first cylinder. Particle diameter 9 nm, and solid volume fraction 2% was used in this study. The heat transfer characteristic of the ferrofluid in the presence and absence of a uniform magnetic field is given in Fig. 3. As can be expected heat flux is enhanced under an applied magnetic field. This fact confirmed experimentally by Jeyadevan et al. (2005). To investigate the effect of natural convection, a set of simulations at the same conditions, but in the absence of any convection was run. Comparison of obtained results showed that in the presence of natural convection heat transfer will increase. Since the temperature gradient in the cylinder was not very high, the difference between two conditions, with and without natural convection, was not significant.

To investigate the effect of natural convection more simulations were performed at temperature difference 40 K and different magnetic fields. Results at $H = 160$ kA/m are presented in Fig. 4, and it is clear that with increase in temperature gradient the effect of natural convection will improve. In addition it is found that the temperature gradient is more effective than the magnetic field on heat transfer of ferrofluids.

Combined effects of temperature gradient and magnetic field's strength were investigated in cylinder 2. In this geometry it is assumed that solid volume fraction is 10%. To estimate heat transfer performance of the ferrofluid, the local Nusselt number, Nu, was calculated at different values of magnetic fields in the presence and absence of natural convection and simulation results are presented in Fig. 5. As can be expected with increase in temperature difference over the cylinder and strength of external magnetic field, heat transfer will improve. It is also found that

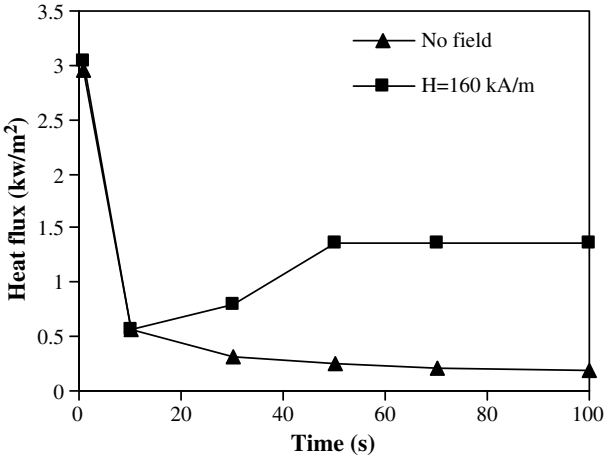

Fig. 3. Effect of magnetic field on heat flux in the presence of natural convection for cylinder 1.

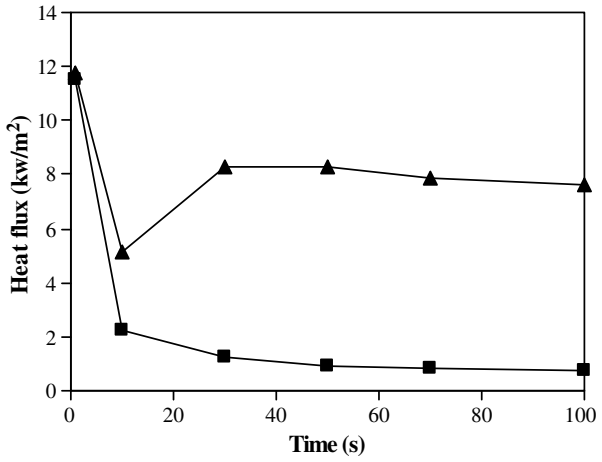

Fig. 4. Heat transfer in the ferrofluid versus time. Triangles and squares show the conditions with and without natural convection for cylinder 1, respectively.

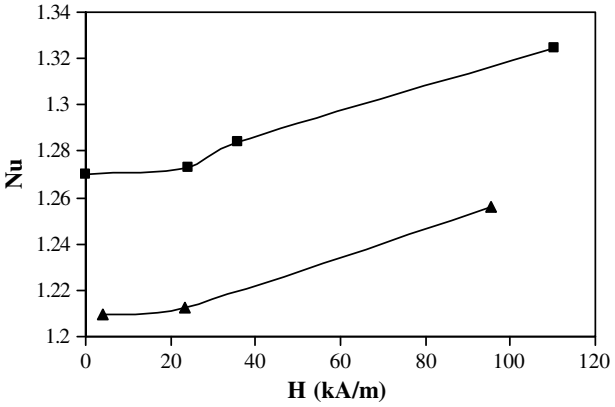

Fig. 5. Nusselt number versus magnetic field strength for cylinder 2. Here $d = 5.5$ nm, and $\Delta T_{\text{critical}} = 25$ K. Triangles and squares belong to $\frac{\Delta T}{\Delta T_{\text{critical}}} = 0.76$ and $\frac{\Delta T}{\Delta T_{\text{critical}}} = 1.52$, respectively.

increasing of H after $H \approx 24$ kA/m will increase heat transfer of the ferrofluid significantly. Note that positive values of $\frac{\Delta T}{\Delta T_{\text{critical}}}$ means that temperature of bottom of the cylinder is higher than the temperature of top of the cylinder, and at $\Delta T > \Delta T_{\text{critical}}$ the convection starts. As Finlayson (1970) reported both buoyancy and magnetic forces can cause the convection. In this work $\Delta T_{\text{critical}}$ is the critical temperature difference for the natural convection due to buoyancy.

According to the estimation of Rosensweig (1997) particle size 10 nm for magnetic fluids is on the threshold of agglomerating. It means that the investigation of effect of particle's diameter on heat transfer of the ferrofluid is important. For the second cylinder similar simulations with higher diameter of magnetic particles were done and results are shown in Fig. 6. According to this figure larger particles decrease heat transfer probably because of the formation of aggregates in the system. In order to obtain better understanding the effect of particle size on transfer phenomena

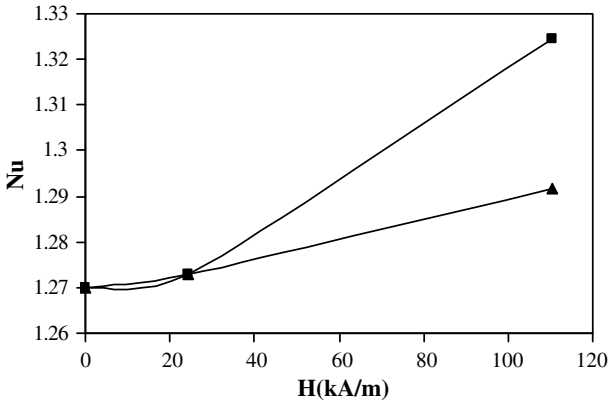

Fig. 6. Nusselt number versus magnetic field strength for cylinder 2. Here $\frac{\Delta T}{\Delta T_{\text{critical}}} = 1.52$, and $\Delta T_{\text{critical}} = 25K$. Triangles and squares belong to $d = 30$ nm and $d = 5.5$ nm, respectively.

flow pattern of the ferrofluid also was studied. As Fig. 7a illustrates in the presence of natural convection for smaller magnetic particles' diameter Rayleigh rolls can be observed. This rotations increase heat transfer, and their effect on thermal convection in ferrofluids is important in certain chemical engineering and biochemical situations (Sunil et al., 2008). For $d = 30$ nm such kind of vortices did not recognize (Fig. 7b).

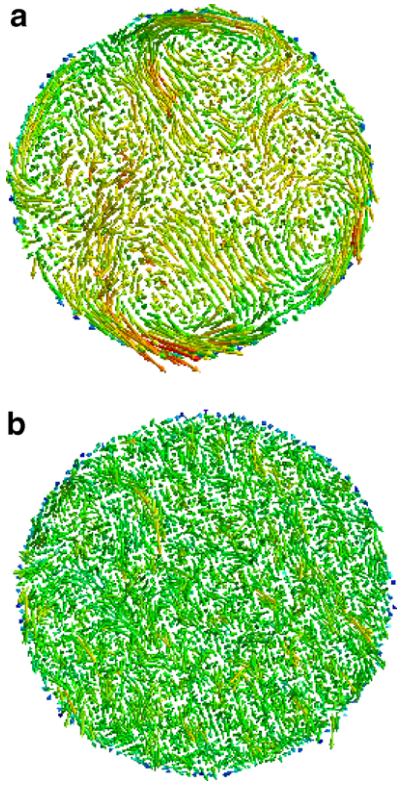

Fig. 7. Velocity vectors in cylinder 2 on a plane at $z = 0.00175$ m, and for $\Delta T_{\text{critical}} = 25$ K, and $\frac{\Delta T}{\Delta T_{\text{critical}}} = 0.76$. (a) $d = 5.5$ nm, and (b) $d = 30$ nm (for interpretation of the references to color in this figure, the reader is referred to the web version of this article).

Number of Rayleigh rolls depends on different parameters such as temperature difference and aspect ratio (length to diameter of cylinder). Any variation of these quantities can induce a change in behavior of the fluid. At aspect ratio 1, magnetic field 160 kA/m, and temperature difference 10 K four rolls have been observed. As Fig. 8 illustrates with passing time the system becomes more stable and symmetric.

Fig. 9 represents fluid streamlines colour coded using velocity magnitude. This kind of vortices observed in the presence of natural convection play an important role in transport mechanism of flow, and increase heat transfer in the system. In the absence of natural convection, this kind of vortices can be observed locally, which means that rolls are close to the domain boundaries. The shape of vortices becomes more uniform in the longer cylinder. It means that the homogeneity inside the cylinder with lower aspect ratio has significant non-uniformity. These results are in good agreement with experimental work done by Sheibani et al. (2003).

To test the effect of magnetic field's direction, a uniform magnetic field in parallel and perpendicular to the direction of temperature gradient has been applied. The velocity profile when the temperature gradient and direction of magnetic field are parallel to each other is shown in Fig. 10. The maximum velocity for the second condition is higher (about 0.009 m/s) than the situation with parallel direction to the temperature gradient. According to the results the heat transfer increases for perpendicular orientation of magnetic field and temperature gradient directions.

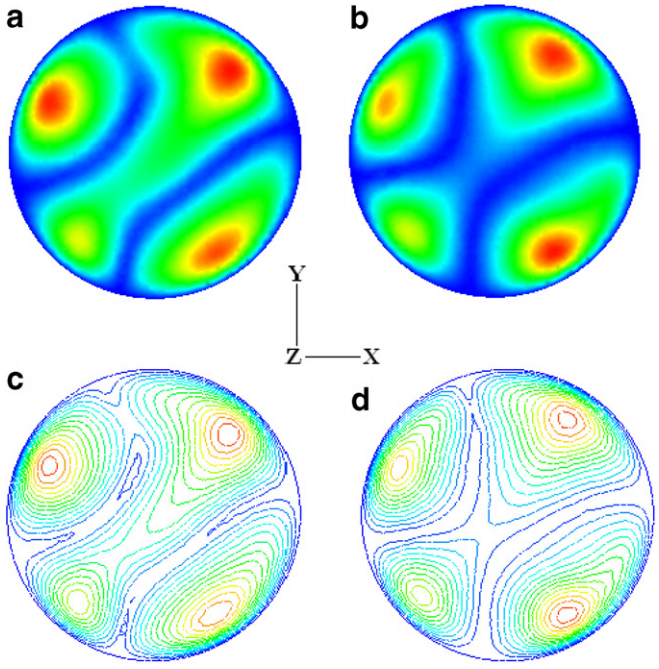

Fig. 8. Rayleigh rolls on a plane at $z = 0.005$ m. The plane is colored with velocity magnitude after (a) 50 s, and (b) 100 s. (c) and (d) show velocity contours at 50 s and 100 s, respectively (for interpretation of the references to color in this figure, the reader is referred to the web version of this article).

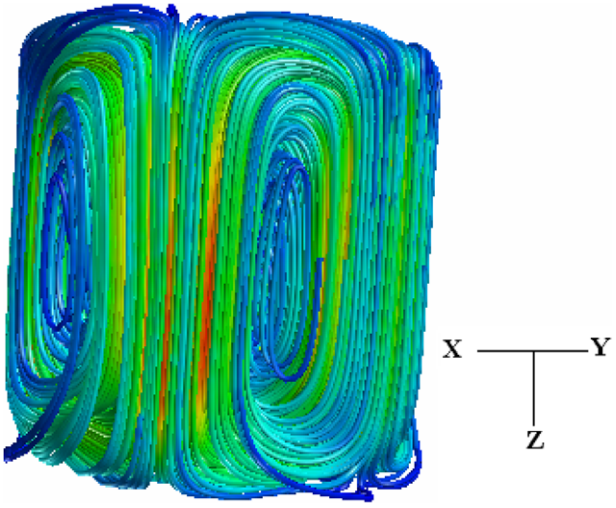

Fig. 9. Fluid streamlines in cylinder 1 at $\mathbf{H} = 160$ kA/m and temperature difference 10 K (for interpretation of the references to color in this figure, the reader is referred to the web version of this article).

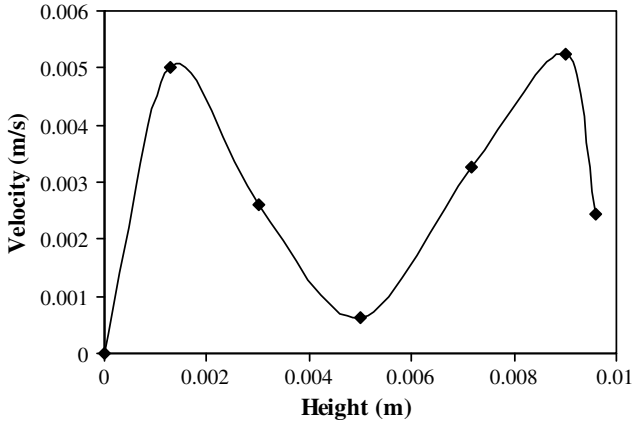

Fig. 10. Velocity of the ferrofluid versus height of the cylinder 1 at $X = 0.0015$ m. Here direction of magnetic field and temperature gradient are parallel.

Velocity profile of ferrofluids depends on some parameters such as type of ferrofluid and strength and direction of magnetic field. More investigation about velocity profiles will be presented in the future work.

5. Conclusion

In this paper heat transfer of a kerosene based ferrofluid in cylindrical geometries is investigated using CFD simulations. It was found that the transferred heat is a function of magnetic field strength and its direction. Results showed that heat transfer can be increased by applying magnetic field perpendicular to the temperature gradient. In addition it was found that increase of magnetic particles' diameter causes generation of colloids in the system and leads to decrease of heat transfer in the ferrofluid.

Acknowledgements

Authors would like to acknowledge the Academy of Finland for the support of this work (Grant No. 110852).

References

Finlayson, B.A., 1970. Convection instability of ferromagnetic fluids. Journal of Fluid Mechanics 40, 753–767.

Jafari, A., Tynjälä, T., Mousavi, S.M., Sarkomaa, P., 2007a. CFD simulation of heat transfer in ferrofluids. In: Proceedings of European Congress of Chemical Engineering, Copenhagen, 16–20 September.

Jafari, A., Tynjälä, T., Mousavi, S.M., Sarkomaa, P., 2008. CFD simulation and evaluation of controllable parameters effect on thermomagnetic convection in ferrofluids using Taguchi technique. Journal of Computers and Fluids. doi:10.1016/j.compfluid.2007.12.003.

Jeyadevan, B., Koganezawa, H., Nakatsuka, K., 2005. Performance evaluation of citric ion-stabilized magnetic fluid heat pipe. Journal of Magnetism and Magnetic Materials 289, 253–256.

Rosensweig, R.E., 1997. Ferrohydrodynamics, second ed. Dover Publications Inc, New York.

Sheibani, H., Liu, Y., Sakai, S., Lent, B., Dost, S., 2003. The effect of applied magnetic field on the growth mechanisms of liquid phase electroepitaxy. International Journal of Engineering Science 41, 401–415.

Snyder, S.M., Cader, T., Finlayson, B.A., 2003. Finite element model of magnetoconvection of a ferrofluid. Journal of Magnetism and Magnetic Materials 262, 269–279.

Strek, T., Jopek, H., 2007. Computer simulation of heat transfer through a ferrofluid. Physica Status Solidi (b) 244 (3), 1027–1037.

Sunil, Chand, P., Bharti, P.K., Mahajan, A., 2008. Thermal convection in micropolar ferrofluid in the presence of rotation. Journal of Magnetism and Magnetic Materials 320, 316–324.

Tangthieng, C., Finlayson, B.A., Maulbetsch, J., Cader, T., 1999. Heat transfer enhancement in ferrofluids subjected to steady magnetic fields. Journal of Magnetism and Magnetic Materials 201, 252–255.

Tynjälä, T., 2005. Theoretical and Numerical Study of Thermomagnetic Convection in Magnetic Fluids. Ph.D. thesis, Lappeenranta University of Technology press, Finland.

Tynjälä, T., Bozhko, A., Bulychev, P., Putin, G., Sarkomaa, p., 2006. On features of ferrofluid convection caused by barometrical sedimentation. Journal of Magnetism and Magnetic Materials 300, e195–e198.

Tynjälä, T., Hajiloo, A., Polashenski, W., Zamankhan, P., 2002. Magnetodissipation in ferrofluids. Journal of Magnetism and Magnetic Materials 252, 123–125.

Tynjälä, T., Ritvanen, J., 2004. Simulations of thermomagnetic convection in an annulus between two concentric cylinders. Indian Journal of Engineering and Material Sciences 11, 283–288.

Xuan, Y., Ye, M., Li, Q., 2005. Mesoscale simulation of ferrofluid structure. International Journal of Heat and Mass Transfer 48 (12), 2443–2451.